Kerr-Schild type initial data for black holes with angular momenta

Claudia Moreno

Center for Gravitational Physics and Geometry, Penn State University, University Park, PA 16802[*]

Darío Núñez

Center for Gravitational Physics and Geometry, Penn State University, University Park, PA 16802[*] *and*
Instituto de Ciencias Nucleares - UNAM, A.P. 70-543,
Ciudad Universitaria, 04510 Mexico, D.F., Mexico[†]

Olivier Sarbach

Department of Physics and Astronomy, Louisiana State University,
202 Nicholson Hall, Baton Rouge, Louisiana 70803–4001[‡]

(Dated: February 7, 2008)

Generalizing previous work we propose how to superpose spinning black holes in a Kerr-Schild initial slice. This superposition satisfies several physically meaningful limits, including the close and the far ones. Further we consider the close limit of two black holes with opposite angular momenta and explicitly solve the constraint equations in this case. Evolving the resulting initial data with a linear code, we compute the radiated energy as a function of the masses and the angular momenta of the black holes.

I. INTRODUCTION

The collision of two black holes is one of the most promising sources for gravitational radiation which the gravitational observatory LIGO will be trying to detect [1].

The detection of gravitational waves is a remarkable project which present challenges in all of their facets, most of them related to the fact that the signal generated from the merging of two black holes will arrive to us as a very tiny ripple in spacetime. Although this is fortunate in the sense that we would not want to have great spacetime disturbances passing all around us, the fact that the signal is so feeble makes essential to the project to be able to theoretically predict and describe with a great deal of accuracy the gravitational wave generated during the process.

The problem of two interacting black holes can be split into three stages, namely: The Newtonian or far limit when they are already interacting gravitationally, but so far from each other that the dynamics can be studied within the Newtonian description. Then, as they get closer, the spacetime begins to be modified and no simplifying assumptions can be used anymore. It is supposed that the gravitational distortions will increase. This period of the evolution is known among the community as the "full 3D" part, meaning that the complete Einstein equations have to be evolved. Finally, in the last stage the two black holes are suppose to merge. After merging, the resulting black hole is supposed to wiggle and giggle, eventually settling down to a stationary black hole. This last part of the process is known as the close limit [2], and its importance resides in the fact that it can be described as a single perturbed black hole. In this case the evolution can be carried out using linearized perturbation theory. For a distorted Schwarzschild or Kerr black hole, the corresponding equations can be cast in a wave-like equation for unconstrained and gauge invariant scalar quantities, and the evolution is much more economic, numerically speaking, than the full 3D evolution.

To solve any system of evolution equations one needs initial data. In general relativity (and gauge theories in general), the initial data cannot be given freely but has to satisfy some constraint equations. There is a wide literature (see [3] and references therein) on how to solve the constraint equations of general relativity. Most approaches are based on the York-Lichnerowicz decomposition [4] in which case the constraint equations are recast in a set of four coupled elliptic equations. These equations simplify considerably if one considers conformally flat initial data, and several interesting solutions which describe a slice with two black holes (see [3] for a review) have been found in this context. However, solutions with conformally flat three-metric suffer from the fact that they cannot exactly represent

Kerr black holes since the Kerr metric is not known to possess a conformally flat space part in the line element, due to the dragging (for a perturbative proof of nonexistence, see [5].) Therefore, this data is likely to contain "junk" radiation which, at least when the two black holes are very far from each other or have merged and settled down to a stationary black hole, might not reflect a realistic astrophysical scenario[18]. More recent proposals relax the requirement for the initial data to be conformally flat [6, 7, 8] and result in new constructions that are able to naturally incorporate spinning black holes.

In the present work, we construct initial data following an approach introduced by Bishop *et al.* [6] and further elaborated in [9, 10] which is not directly based on the York-Lichnerowicz decomposition. The advantage of this approach is that one can easily obtain closed analytic expressions for the solution to the constraint equations in some limiting cases, including the close limit approximation. The approach, which is briefly reviewed in Sec. II, uses a Kerr-Schild type of metric in order to construct the initial data. While in [6] the superposition of two Schwarzschild black holes is discussed, we generalize their proposal to spinning black holes in Sec. III. Our superposition has some appealing features (described in more detail in Sec. III): i) Far limit: When the two black holes are infinitely far from each other, one obtains in the region near each one of them, initial data describing a single Kerr black hole. ii) Close limit: When the black holes "sit on the top of each other", one obtains again a single Kerr black hole.

In Sec. IV we consider the close limit regime in which two rotating holes are close to each other with their singularities enclosed by a common apparent horizon. In this case, the initial slice can be viewed as a distorted $t = const.$ Kerr slice in Kerr-Schild coordinates. We explicitly solve the linearized constraint equations for the case in which the angular momenta of the two holes are opposite but equal in magnitude. Using a generalized version [11] of the Zerilli and Regge-Wheeler equations, we evolve our initial data in Sec. V and compute the radiated energy. In particular, we discuss the dependence of the energy on the angular momenta of the holes and compare our results to other calculations based on Bowen-York data [12]. We conclude with a summary and remarks in Sec. VI and include technical details in appendices A and B.

II. KERR-SCHILD INITIAL DATA

Let us briefly review Bishop *et al.*'s proposal [6] to solve the constraint equations of general relativity: The assumption is that at the initial slice, the metric and its time derivative are of Kerr-Schild type,

$$ds^2 = (\eta_{\mu\nu} + 2\,V\,l_\mu\,l_\nu)dx^\mu dx^\nu, \tag{1}$$

where $\eta_{\mu\nu}$ is the flat metric, $\eta_{\mu\nu}dx^\mu dx^\nu = dt^2 - dx^2 - dy^2 - dz^2$, V is a function and l_μ a covector which is null, normalized such that $l_t = -1$ (as a consequence, $\delta^{ij}l_i l_j = 1$ and l_i has only two independent components). The three metric and extrinsic curvature with respect to a slice $t =$const. are

$$g_{ij} = \delta_{ij} - 2Vl_il_j\,, \tag{2}$$

$$K_{ij} = -\frac{1}{\alpha}(Vl_il_j)_{,t} + \alpha[2Vl^c(Vl_il_j)_{,c} - (Vl_i)_{,j} - (Vl_j)_{,i}], \tag{3}$$

where $\alpha = 1/\sqrt{1-2V}$ is the lapse and where $i = x, y, z$ refer to Cartesian coordinates. The way Bishop *et al.* propose to solve the constraints is to make an ansatz for the (spatial part) of the null vector l_μ, to insert the equations (2) and (3) into the Hamilton and momentum constraint equations and to solve the resulting set of four coupled differential equations for the unknowns V, $\dot{V} \equiv \partial_t V$ and $\dot{l}_i \equiv \partial_t l_i$. In [6], a procedure is given for how to solve the nonlinear constraint equations for the superposition of two non-spinning black holes. In the close limit approximation (i.e. in the limit where the distance between the two black holes is much smaller than the mass of the holes) the constraint equations can even be solved analytically [9].

Below, we first generalize Bishop *et al.*'s ansatz for l_i to include the superposition of spinning black holes. Then, we solve the constraint equations in the close limit approximation. For simplicity, we will only consider the case where the angular momentum of the two black holes are opposite but equal in magnitude. In this case, one obtains a perturbed Schwarzschild black hole which is easier to study than a perturbed Kerr black hole.

III. SUPERPOSING TWO KERR BLACK HOLES

In Cartesian Kerr-Schild coordinates, the Kerr spacetime can be written in the form (1) with

$$V = -\frac{M\,R^3}{R^4 + a^2\,z^2}\,, \tag{4}$$

$$l_\mu = \left(-1, -\frac{R\,x + a\,y}{R^2 + a^2}, -\frac{R\,y - a\,x}{R^2 + a^2}, -\frac{z}{R}\right)\,, \tag{5}$$

where R is a positive function with units of distance given by

$$R^2 = \frac{1}{2} \left(\|\vec{x}\|^2 - a^2 + \sqrt{(\|\vec{x}\|^2 - a^2)^2 + 4a^2 z^2} \right). \tag{6}$$

Here, M and a denote the ADM mass and the rotational parameter, respectively. Note that R is well-defined outside the disc $\|\vec{x}\|^2 \leq a^2$, $z = 0$, whose boundary is the ring singularity.

In order to generalize Bishop *et al.*'s proposal to spinning black holes, we first notice that the spatial part of the null covector given in Eq. (5) can be rewritten as the sum of two covectors:

$$l_i = l_i^{(1)} + l_i^{(2)},$$

where

$$\vec{l}^{(1)} = -\left(\frac{R\,x}{R^2 + a^2}, \frac{R\,y}{R^2 + a^2}, \frac{z}{R} \right),$$

$$\vec{l}^{(2)} = -a\left(\frac{y}{R^2 + a^2}, -\frac{x}{R^2 + a^2}, 0 \right).$$

Here and in the following, we identify l_i with $l^i = \delta^{ij} l_j$ and denote by $\vec{l}$ the vector (l^x, l^y, l^z). As in the Schwarzschild case [6], the vector $\vec{l}^{(1)}$ can be written as the gradient of a potential function,

$$\vec{l}^{(1)} = N\,\vec{\nabla}\Phi,$$

where N is a normalization function, and

$$\Phi = \frac{M}{R}.$$

Now, the vector $\vec{l}^{(2)}$, which vanishes in the non-spinning case, can be written as the cross product of $\vec{l}^{(1)}$, that is, of $N\,\vec{\nabla}\Phi$ (with the same normalization function), and a vector proportional to the angular momentum of the black hole:

$$\vec{l}^{(2)} = -N\,\frac{\vec{a}}{R} \times \vec{\nabla}\Phi,$$

where $\vec{a} = (0, 0, a)$. If we allow $\vec{a}$ to have components in arbitrary directions and replace $a \cdot z$ by $\vec{a} \cdot \vec{x}$ in the expressions (4) and (6), we obtain the Kerr solution for general angular momentum $\vec{J} = M\vec{a}$.

Thus, the spatial part of the covector l_μ can be written as

$$\vec{l} = N \left(\vec{\nabla}\Phi + \vec{\nabla} \times \vec{b} \right), \tag{7}$$

where the potential Φ is given by

$$\Phi = \frac{M}{R},$$

and

$$\vec{b} = \frac{M\,\vec{a}}{2R^2},$$

where now

$$R^2 = \frac{1}{2} \left(\|\vec{x}\|^2 - \|\vec{a}\|^2 + \sqrt{(\|\vec{x}\|^2 - \|\vec{a}\|^2)^2 + 4(\vec{a} \cdot \vec{x})^2} \right).$$

Using the linearity of the ∇ operator, we have the necessary basis to propose the following ansatz for the spatial part of the null vector, that is, for the description of a Cauchy slice with characteristics that allow a description of two black holes.

Let the black holes have masses M_1, M_2, and angular momenta $\vec{J}_1 = M_1 \vec{a}_1$, $\vec{J}_2 = M_2 \vec{a}_2$, respectively and their centers be at the points $\vec{x}_1$, for black hole one, and at $\vec{x}_2$, for black hole two. Having written a single Kerr black hole in the form (7), it is not difficult to generalize Bishop *et al.*'s proposal: We propose

$$\Phi = \frac{M_1}{R_1} + \frac{M_2}{R_2}, \tag{8}$$

$$\vec{b} = \frac{1}{2} \left(\frac{M_1 \vec{\tilde{a}}_1}{R_1^2} + \frac{M_2 \vec{\tilde{a}}_2}{R_2^2} \right), \tag{9}$$

with

$$R_i^2 = \frac{1}{2} \left(\|\vec{x} - \vec{x}_i\|^2 - \|\vec{\tilde{a}}_i\|^2 + \sqrt{\left(\|\vec{x} - \vec{x}_i\|^2 - \|\vec{\tilde{a}}_i\|^2 \right)^2 + 4 \left(\vec{\tilde{a}}_i \cdot (\vec{x} - \vec{x}_i) \right)^2} \right), \tag{10}$$

$$\vec{\tilde{a}}_i = (1 - \vartheta(d)) \, \vec{a}_i + \vartheta(d) \, \vec{a}_f, \tag{11}$$

where $d = \|\vec{x}_1 - \vec{x}_2\|$ is the "distance" between the black hole's centers, $i = 1, 2$, and $\vartheta(d)$ is an interaction function between the angular momenta of each black hole. Its specific form can be left undetermined for the moment, as for the present analysis it is enough that it is a smooth function which behaves in the following way:

$$\lim_{d \to 0} \vartheta(d) \to 1,$$
$$\lim_{d \to \infty} \vartheta(d) \to 0.$$

There are several well known functions with this type of behavior. The specific form of $\vartheta(d)$ might be related with the spin-spin interactions of particle physics, and will be analyzed in future works.

The final rotational parameter $\vec{a}_f$ is given by

$$\vec{a}_f = \frac{M_1 \, \vec{a}_1 + M_2 \, \vec{a}_2}{M_1 + M_2}, \tag{12}$$

which corresponds to the vector addition of the angular momenta, $\vec{J}_f = \vec{J}_1 + \vec{J}_2$. We will see shortly that Eq. (12) is a necessary condition for obtaining the correct close limit.

Finally, we comment on the fact that our ansatz has potential problems at points where $\vec{k} \equiv \vec{\nabla}\Phi + \vec{\nabla} \times \vec{b}$ vanishes (such that $\vec{l}$ cannot be normalized at these points). For the superposition of two Schwarzschild black holes, there is exactly one such point. For two Kerr black holes with $M_1 = M_2$ and $\vec{a}_1 = -\vec{a}_2$, we found that $\vec{k}$ is singular at $\vec{x} = \frac{\vec{x}_1}{\|\vec{x}_1\|} \times \vec{a}_1$, where the two holes are centered at $\vec{x}_1$, $\vec{x}_2 = -\vec{x}_1$. In the situation studied in the next section we will see that this singularity does not cause any problems since there, we can excise a region which contains the ring singularities of the two holes and the above singularity.

Besides its mathematical simple form, the above ansatz has the following useful limits:

1. Far limit: Let us consider that the center of the black hole 1 is at the origin, and that the center of the other is far from the origin, that is, $\|\vec{x}_2\|$ goes to infinity. Since then $\vartheta(d) = 0$, we obtain from Eq.(11) that $\vec{\tilde{a}}_i = \vec{a}_i$. So from equation Eq.(10), we see that each R_i^2 depends only on the parameters of the respective black hole. Furthermore, in the vicinity of black hole 1, R_2 is very large compared to R_1 so the second terms in Eqs.(8,9) can be dropped and one obtains the l_i for one black hole with mass M_1 and angular momentum $\vec{J}_1 = M_1 \vec{a}_1$.

2. Close limit: Suppose that $\vec{x}_1 = \vec{x}_2$, i.e. the limiting case when the distance d between the two holes goes to zero. In this case, $\vartheta(d) = 1$, and $\vec{\tilde{a}}_1 = \vec{\tilde{a}}_2 = \vec{\tilde{a}}_f$, so $R_1 = R_2$. Taking into account the expression for the final angular momentum, Eq.(12), the potential Φ, and the vector $\vec{b}$, Eqs.(8,9), we see that one obtains one black hole with center at $\vec{x}_1$, mass $M = M_1 + M_2$, and angular momentum $M \vec{a} = M_1 \vec{a}_1 + M_2 \vec{a}_2$.

3. One hole limit: If the mass of one black hole, say M_2, vanishes, it can be seen from Eq.(12) that $\vec{a}_f = \vec{a}_1$ thus, from Eq.(11), $\vec{\tilde{a}}_i = \vec{a}_i$. Thus the function R_1 only depends on $\vec{a}_1$ and the potential Φ, and the vector $\vec{b}$, Eqs.(8,9), reduce to the expressions corresponding to black hole 1.

4. Schwarzschild limit: Finally, our ansatz reduces to the one given by Bishop *et al.* in the non-spinning case $\vec{a}_1 = \vec{a}_2 = \vec{0}$.

Thus, we consider that we are presenting an educated ansatz for initial data with certain attractive properties describing the null vector on a space-like slice with two rotating black holes. In order to complete the initial data, we have to solve the constraint equations to yield the function V, and the time derivatives of V and l_i. We discuss this below, where we explicitly solve the constraint equations in the close limit approximation, where the distance d between the two holes is infinitesimal. For simplicity, we will also assume that the angular momenta of the holes are equal in magnitude but opposite, obtaining a non-spinning black hole when $d = 0$ (see figure 1).
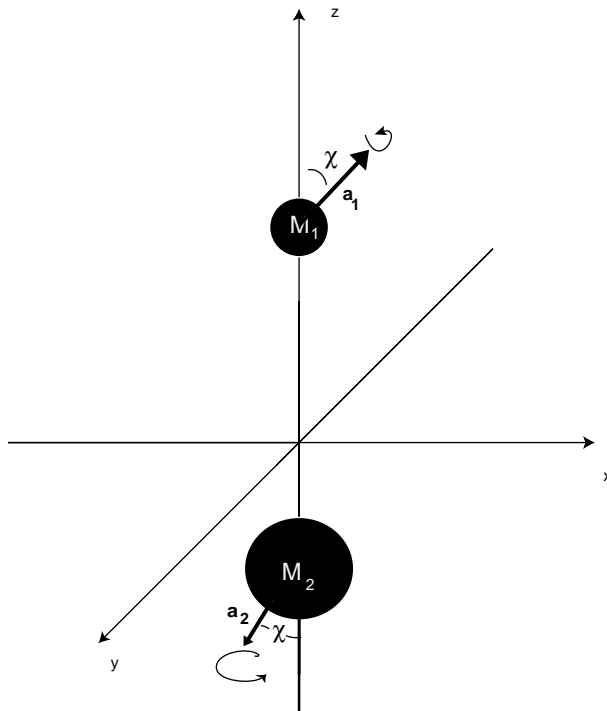
IV. MODEL FOR "KERR+KERR=SCHWARZSCHILD"

FIG. 1: Initial data representing two rotating black holes, such that the merger is a non rotating one.

We expand Φ and $\vec{b}$ in Eqs. (8,9), in terms of the dimensionless "distance" between the black holes,

$$\epsilon = \frac{d}{M_1 + M_2},$$

which we consider to be small compared to unity. In the following, we choose the Cartesian coordinates such that the two holes are located at $\vec{x}_1 = (0, 0, M_2\epsilon)$ and $\vec{x}_2 = (0, 0, -M_1\epsilon)$, respectively. This "center of mass condition" $(M_1\vec{x}_1 + M_2\vec{x}_2 = \vec{0})$ on the coordinate system simplifies the calculations below since no terms proportional to ϵ will appear in the expansions[19]. Similarly, we shall write $\vec{a}_1 = M_2 s\hat{e}$, and $\vec{a}_2 = -M_1 s\hat{e}$, where $\hat{e}$ is a unit vector, and s a dimensionless parameter equal to $J_1/M_1 M_2$. As a consequence of this, $\vec{a}_f$ is equal to zero (see Eq. (12)), thus to zeroth order in ϵ, we have a Schwarzschild black hole.

Using this and the Taylor expansion

$$\vartheta(\epsilon) = 1 + \vartheta'(0)\epsilon + \frac{1}{2}\vartheta''(0)\epsilon^2 + \mathcal{O}(\epsilon^3),$$

for the "spin–spin interaction" function, we eventually arrive at the following expansions for Φ and $\vec{b}$

$$\Phi = \frac{M}{r} + \frac{M M_1 M_2}{2r^3}\left[3\cos^2\theta - 1 + q^2\left(1 - (\hat{e}\cdot\hat{x})^2\right)\right]\epsilon^2 + \mathcal{O}(\epsilon^3), \tag{13}$$

$$\vec{b} = -\frac{M M_1 M_2}{r^3}q\cos\theta\,\hat{e}\,\epsilon^2 + \mathcal{O}(\epsilon^3), \tag{14}$$

where $M = M_1 + M_2$ is the total mass, and where we have introduced $r = \|\vec{x}\|$, $\hat{x} = \vec{x}/r$, $\cos\theta = z/r$. Here, $q = s\vartheta'(0)$ is proportional to the dimensionless angular momentum parameter s introduced above. The proportionality factor depends on the slope of the interpolation function $\vartheta(d)$ at $d = 0$. Since $\vartheta(0) = 1$ and $\vartheta(r) \to 0$ as $r \to \infty$ a natural choice for this factor is $\vartheta'(0) = -1$ in which case $q = -s$. Note that for the superposition of non-extremal black holes, we have $|s| < 1$.

To summarize, the expansion depends on the parameters: M_1, M_2 (which are supposed to model the masses of the black holes), $q = -s$ (the dimensionless angular momentum parameter) and $\hat{e}$ (the orientation of the angular momentum with respect to the common axis of the holes).

In order to proceed, it is convenient to expand the above expressions in terms of spherical harmonics. Since the quantities we consider are real, we choose the real harmonics $(Y^{\ell 0}, R^{\ell m}, I^{\ell m})$, $m = 1, ..., \ell$, defined in Appendix A. Parameterizing $\hat{e} = (0, \sin\chi, \cos\chi)$ without loss of generality and using Eq. (7), the spatial vector $\vec{l}$ eventually assumes the form (see Appendix A for more details)

$$
\begin{aligned}
l_r &= -1 + \mathcal{O}(\epsilon^3), \\
l_A &= \frac{M_1 M_2}{r}\partial_A \left[\gamma_{20} Y^{20} + \gamma_{2-1} I^{21} + \gamma_{22} R^{22} + \gamma_{11} R^{11}\right] \epsilon^2 \\
&+ \frac{M_1 M_2}{r}\hat{\varepsilon}_A^B \partial_B \left[\delta_{20} Y^{20} + \delta_{2-1} I^{21}\right] \epsilon^2 + \mathcal{O}(\epsilon^3).
\end{aligned}
\tag{15}
$$

where $A = \theta, \phi$ denote the angular variables and $\hat{\varepsilon}_A^B$ denotes the Levi-Civita tensor with respect to the standard metric on S^2. The constant coefficients $\gamma_{\ell m}$ and δ_{lm} are given by

$$
\begin{aligned}
\gamma_{20} &= \sqrt{\frac{4\pi}{5}}\left[1 + \frac{q^2}{6}\left(1 - 3\cos^2\chi\right)\right], \\
\gamma_{2-1} &= -\sqrt{\frac{\pi}{15}}\, q^2 \sin(2\chi), \\
\gamma_{22} &= \sqrt{\frac{\pi}{15}}\, q^2 \sin^2\chi, \\
\gamma_{11} &= -\sqrt{\frac{4\pi}{3}}\, q \sin\chi, \\
\delta_{20} &= \sqrt{\frac{64\pi}{45}}\, q \cos\chi, \\
\delta_{2-1} &= \sqrt{\frac{16\pi}{15}}\, q \sin\chi.
\end{aligned}
\tag{16}
$$

A nice feature of our ansatz is that the only contributions with $\ell < 2$ are in the even-parity sector with $\ell = 1$, and this sector is known to contain only gauge modes (see, for instance, Ref. [11] for a proof of this statement). Thus, to first order in ϵ^2, we have no change in the mass nor in the (total) angular momentum. It is also interesting to notice that the even-parity contributions look exactly as in the non-spinning case (see [6, 9]), except that we have to replace in each sector $M_1 M_2$ by $\gamma_{2m} M_1 M_2$ (and for $q = 0$ all the γ_{2m}'s vanish except for γ_{20}, in which case we recover the ansatz in the non-spinning case.)

In order to solve the constraint equations, we expand

$$
\begin{aligned}
V &= -\frac{M}{r} + \epsilon^2 \left[v_{20}(r) Y^{20} + v_{2-1}(r) I^{21} + v_{22}(r) R^{22}\right] + \mathcal{O}(\epsilon^3), \\
\dot{V} &= \epsilon^2 \left[\dot{v}_{20}(r) Y^{20} + \dot{v}_{2-1}(r) I^{21} + \dot{v}_{22}(r) R^{22}\right] + \mathcal{O}(\epsilon^3), \\
\dot{l}_A &= \epsilon^2 \partial_A \left[\dot{k}_{20}(r) Y^{20} + \dot{k}_{2-1}(r) I^{21} + \dot{k}_{22}(r) R^{22}\right] \\
&+ \epsilon^2 \hat{\varepsilon}_A^B \partial_B \left[\dot{n}_{20}(r) Y^{20} + \dot{n}_{2-1}(r) I^{21}\right] + \mathcal{O}(\epsilon^3),
\end{aligned}
\tag{17}
$$

where $v_{2m}(r)$, $\dot{v}_{2m}(r)$ and $\dot{n}_{2m}(r)$ are unknown functions. Introducing (15) and (17) into the constraint equations, and keeping only terms of the order ϵ^2, we obtain a set of linear inhomogeneous differential equations for these amplitudes, where the inhomogeneity is given by the coefficients in the expansion (15). These equations split into two sets – one set comprising the even-parity amplitudes v_{2m}, $\dot{v}_{2m}$, $\dot{k}_{2m}$, and the other set comprising the odd-parity amplitude $\dot{n}_{2m}$. Amplitudes belonging to different m's also decouple because the background is spherically symmetric.

As observed above, the coefficients in the expansion of l_A in terms of spherical harmonics with even parity are proportional to $\gamma_{2m} M_1 M_2$. Since we have already solved the constraint equations in the non-spinning case, for which

$\gamma_{20} = \sqrt{4\pi/5}$ while all other γ_{2m}'s vanish, the solution to the constraint equations is the same as in the non-spinning case [9] except that we have to rescale in each sector $M_1 M_2$ by γ_{2m}. The result is

$$v_{2m}(x) = -\gamma_{2m}\frac{2\mu}{3}\left(1 - \frac{2}{x} + \frac{3}{x^2} + \frac{3}{x^3} + \frac{6\pi}{x^2}Y_4(i\sqrt{24/x})\right) + \gamma_{2m}\frac{\mu C_{2m}}{x^2}J_4(i\sqrt{24/x}), \tag{18}$$

where $x = r/M$, $\mu = M_1 M_2/M^2$ is the dimensionless reduced mass of the system, and C_{2m} are free constants. The factor 6π in front of the Bessel function Y_4 ensures that the initial data is asymptotically flat. The amplitudes $\dot{v}_{2m}$ and $\dot{k}_{2m}$ are obtained from Eqs. (6) and (7) of Ref. [9], where, again, one has to replace $M_1 M_2$ by $\gamma_{2m}M_1 M_2$.

In the odd parity sector, the constraints yield

$$\dot{n}_{2m}(x) = \delta_{2m}\frac{\mu \hat{C}_{2m}}{x},$$

where $\hat{C}_{2m}$ are other free constants.

At this point, a question that arises is what meaning can be given to the free constants C_{2m} and $\hat{C}_{2m}$. As discussed in [6, 9], the constants C_{2m} can be used in order to fix the position of the apparent horizon (AH) to its background value $x = 2$: To leading order in ϵ, the position of AH is given by the image of the circle $x = 2$ under the map

$$\vec{x} \mapsto \vec{x} - \epsilon^2 D(\vec{x})\frac{\vec{x}}{x},$$

where the deviation function $D(\vec{x})$ is given by

$$D(\vec{x}) = -\frac{3}{7}\sum_m \left(\frac{4}{3}v_{2m}(x=2) - \gamma_{2m}\mu\right)Y^{2m}(\vartheta, \varphi).$$

The induced metric on the AH is

$$g_{AH} = 4M^2 \left(1 + \epsilon^2 D(x=2)\right)\left(d\vartheta^2 + \sin^2\vartheta\, d\varphi^2\right).$$

Since the corresponding scalar curvature is

$$R_{AH} = \frac{1}{4M^2}\left(2 + 4\epsilon^2 D(x=2)\right),$$

we see that the constants C_{2m} describe the deformation of the AH. There is no physical preferred choice, but for definiteness, we will choose C_{2m} such that $D(x=2)$ vanishes, i.e. such that the AH is not deformed.

A geometrical interpretation of the constants $\hat{C}_{2m}$ can be given as follows: In the presence of an axial Killing field ∂_φ ($\varphi \in (0, 2\pi)$), we can define the quantity

$$J(r) = \frac{1}{16\pi}\int_{S_r} *\left(dg_{\varphi\mu} \wedge dx^\mu\right), \tag{19}$$

where S_r denotes a spatial sphere of radius r and $*$ is the Hodge dual. For $r \to \infty$ this gives the Komar angular momentum. For an axialsymmetric spacetime with Killing horizon at $r = r_H$, $J(r_H)$ gives the angular momentum of the horizon. For a Schwarzschild black hole, $J(r = 2M) = 0$. Although the Komar formula does not make sense if ∂_φ is not an axial Killing field, we can linearize Eq. (19) around a Schwarzschild black hole, evaluate the resulting expression at the AH, and interpret the resulting quantity as the "angular momentum of the AH" [20]. For $\ell = 2$, the result is

$$J(r = 2M) = \epsilon^2 \frac{3M}{\pi}\sum_m \phi_{2m}(x=2)\int \cos\vartheta\, Y^{2m}d\Omega, \tag{20}$$

where ϕ_{2m} are the gauge invariant amplitudes given in the next section. However, since $\cos\vartheta$ is proportional to Y^{10}, all the spherical integrals vanish by virtue of the orthogonality of the spherical harmonics. Nevertheless, it seems reasonable to associate the gauge-invariant quantities $\phi_{2m}(x=2)$ with a measure for the differential rotation of the AH. Since these quantities depend on $\hat{C}_{2m}$ (see below), the constants $\hat{C}_{2m}$ can be used in order to control the amount of this differential rotation. Again, there is no physically preferred choice for the amount of differential rotation. For definiteness, we will choose $\hat{C}_{2m}$ such that $\phi(x=2)$ vanishes.

V. NUMERICAL EVOLUTION

Here, we evolve the initial data obtained in the previous section using the linearized Einstein equations. We compute the radiated energy at infinity and compare with other results. Since the background metric is Schwarzschild in Kerr-Schild coordinates, we can use the generalized versions of the equations of Zerilli and Regge-Wheeler (RW) derived in Ref. [11] in order to perform the evolution. Expressing these equations in Kerr-Schild coordinates, we have, for the case of interest $\ell = 2$,

$$\ddot{\psi} - \frac{x-2}{x+2}\psi'' - \frac{2}{x(x+2)}(\psi' - \dot{\psi}) - \frac{4}{x+2}\dot{\psi}' + \frac{6(3 + 6x + 4x^2 + 4x^3)}{x^2(x+2)(3+2x)^2}\psi = 0, \tag{21}$$

$$\ddot{\phi} - \frac{x-2}{x+2}\phi'' - \frac{2}{x(x+2)}(\phi' - \dot{\phi}) - \frac{4}{x+2}\dot{\phi}' + \frac{6(x-1)}{x^2(x+2)}\phi = 0, \tag{22}$$

where ψ and ϕ denote the Zerilli and the RW amplitude, respectively, and where a dot and a prime denote derivatives with respect to the dimensionless coordinates t/M and $x = r/M$, respectively.

In order to evolve these equations, we have to give initial data to ψ, $\dot{\psi}$ and ϕ, $\dot{\phi}$. We can construct those from the linearized three metric and extrinsic curvature using the formulas given in Sec. III of Ref. [11]. The three metric and extrinsic curvature can be obtained from the expressions (2, 3). The final result is

$$\psi_{2m} = M\left[\frac{x^3 v_{2m} - 6\gamma_{2m}\mu}{3x(2x+3)}\right],$$

$$\dot{\psi}_{2m} = -M\left[\frac{2x^3(2x-1)v_{2m} + x^4(x-2)v'_{2m} + 6\gamma_{2m}\mu(x-1)}{6x^2(2x+3)}\right].$$

where v_{2m} is given in Eq. (18), and

$$\phi_{2m} = -2M\mu\delta_{2m}\left(\frac{1}{x^2} + \frac{\hat{C}_{2m}}{4x}\right),$$

$$\dot{\phi}_{2m} = \frac{2M\mu\delta_{2m}}{x^3}.$$

Here, we choose the constants C_{2m} and $\hat{C}_{2m}$ to be

$$C_{2m} = 2.7, \qquad \hat{C}_{2m} = -2, \tag{23}$$

which insures that the AH is not deformed and shows no differential rotation, as discussed in the previous section.

An expression for the radiated energy in terms of gauge-invariant quantities is given in [11]. In our case ($\ell = 2$), this energy takes the form

$$\frac{dE}{du} = \frac{3}{2\pi M^2}\sum_m\left(\dot{\psi}_{2m}^2 + \dot{\phi}_{2m}^2\right),$$

where $\dot{\psi}$ and $\dot{\phi}$ are evaluated in the radiative zone. (Note that the radiated angular momentum is zero in our case since both the initial and the final stage have zero total angular momentum.) Given the linearity of the equations and the form of the initial data, the dependence of the time derivatives of the Zerilli and RW functions are

$$\dot{\psi}_{2m}(t,r) = \epsilon^2\mu M\,\gamma_{2m}\,\dot{\psi}_0(t,r),$$

$$\dot{\phi}_{2m}(t,r) = \epsilon^2\mu M\,\delta_{2m}\,\dot{\phi}_0(t,r),$$

where the functions ψ_0 and ϕ_0 are dimensionless. Accordingly, the total radiated energy is

$$E(q,\chi) = M\epsilon^4\mu^2\left[c_{even}\,E_{even} + c_{odd}\,E_{odd}\right], \tag{24}$$

where

$$E_{even} = \int_0^\infty \dot{\psi}_0^2\,\frac{dt}{M}, \qquad c_{even} = \frac{3}{2\pi}\left(\gamma_{20}^2 + \gamma_{2-1}^2 + \gamma_{22}^2\right),$$

$$E_{odd} = \int_0^\infty \dot{\phi}_0^2\,\frac{dt}{M}, \qquad c_{odd} = \frac{3}{2\pi}\left(\delta_{20}^2 + \delta_{2-1}^2\right).$$

Using the expressions (16), we obtain, after some simplifications,

$$c_{even} = \frac{6}{5}\left[\left(1 - \frac{q^2}{3}\right)^2 + q^2 \sin^2\chi\right],$$

$$c_{odd} = \frac{8q^2}{15}\left[4 - \sin^2\chi\right].$$

Since E_{even} and E_{odd} do not depend on the angle χ, we can easily derive the expressions for the extrema of the radiated energy, Eq.(24) with respect to the angle χ:

$$\frac{\partial E}{\partial \chi} = M\epsilon^4\mu^2\, E_{even}\, \frac{6q^2}{5}\left(1 - \frac{4}{9}\Upsilon\right)\sin(2\chi),$$

$$\frac{\partial^2 E}{\partial \chi^2} = M\epsilon^4\mu^2\, E_{even}\, \frac{12q^2}{5}\left(1 - \frac{4}{9}\Upsilon\right)\cos(2\chi),$$

where $\Upsilon = \frac{E_{odd}}{E_{even}}$. Thus, we see that the extrema are at $\chi = 0, \frac{\pi}{2}$, and provided that $E_{even} < \frac{4}{9}E_{odd}$, the maximum of the energy radiated will be when the angular momentum of the black holes are parallel to the approaching axis, and the minimum will be when the angular momentum is perpendicular to it. Fixing C_{2m} and $\hat{C}_{2m}$ according to Eq. (23), a numerical evolution using a first order reformulation of the equations (21,22) described in Appendix B yields (to 1.5% accuracy)

$$E_{even} = 1.74 \times 10^{-4}, \qquad \frac{4}{9}E_{odd} = 1.78 \times 10^{-3},$$

so the minimum of the radiated energy is at $\chi = \pi/2$. The fact that $4E_{odd}/9$ is much larger than E_{even} suggests that this will also be the case for different values of C_{2m} and $\hat{C}_{2m}$, as long as these do not differ much from the values chosen here.
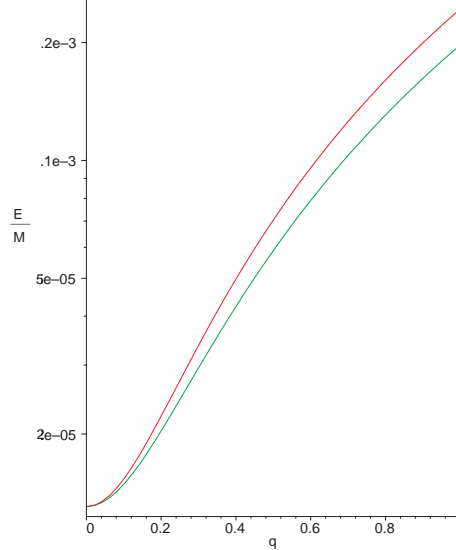

FIG. 2: The radiated energy as a function of the angular momenta for two cases: The upper curve corresponds to the case when the angular momentum of the black holes are parallel to the approaching axis ($\chi = 0$), and the lower one when it is perpendicular to it ($\chi = \pi/2$). Here, we have set $\epsilon = 1$ and $\mu = 1/4$.

Notice that once E_{even} and E_{odd} have been computed numerically, the radiated energy can be obtained for *any* values of the angular momentum number q and the angular momentum orientation angle χ by using Eq. (24). This function is illustrated in the figures 2 and 3. The dependence on the angle χ is much more noticeable when the angular momentum per square mass of the black holes is large. The maximum radiated energy for a fixed total mass and separation is given by

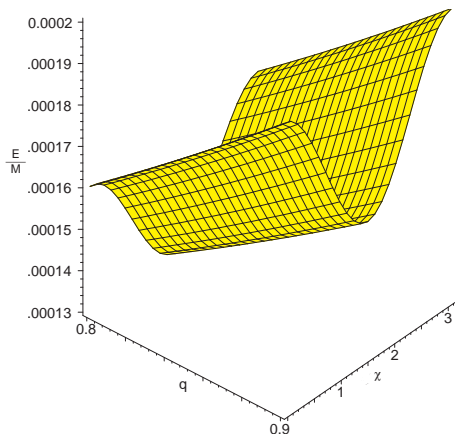$$E \leq E(q=1, \chi=0) = M\epsilon^4 \times 5.4 \times 10^{-4}.$$

FIG. 3: Dependence of the energy radiated on the angle between the angular momenta of the black holes and the approaching axis, for values of q close to the extremal case. Here, $\epsilon = 1$ and $\mu = 1/4$.

Our results on the energy radiated agree qualitatively with those presented recently by Khanna [12]. There, the physical situation sketched in figure 1 is modeled using Bowen-York initial data in the close-slow approximation. It is interesting to notice that the quantities we have identified with a measure for the differential rotation of the AH also vanish in the initial data used in [12] since there, perturbations with odd parity are trivial. In particular, Khanna also obtains that there is more radiated energy for $\chi = 0$ than for $\chi = \pi/2$. However in [12], the initial data depends linearly on q, so the radiated energy depends only quadratically on q whereas in our initial data, the dependence on q is more complicated. In particular, we have a contribution in both the even and the odd parity sectors.

VI. SUMMARY AND CONCLUDING REMARKS

We have made an ansatz to give initial data representing the superposition of two Kerr black holes. The ansatz depends on the parameters M_i (masses), $\vec{J}_i$ (angular momentum), and an (unphysical) distance d between the two black holes. The ansatz is such that when d goes to infinity, one obtains two Kerr black holes in Kerr-Schild coordinates with masses M_i and angular momentum $\vec{J}_i$. Furthermore, when $d = 0$, one obtains one Kerr black hole in Kerr-Schild coordinates with parameters $M = M_1 + M_2$, and $\vec{J} = \vec{J}_1 + \vec{J}_2$.

The ansatz superposes two black holes with vanishing linear momentum, and a natural question is whether or not we can generalize our proposal to boosted black holes. In their paper [6], Bishop *et al.* indicate how to superpose two boosted Schwarzschild black holes: There, one can replace the potential $\Phi(\vec{x}) = 1/|\vec{x}|$ by a more complicated expression $\Phi_{\vec{v}}(\vec{x})$ that depends on the speed, $\vec{v}$, of the boost. A proposal for two boosted non-spinning black holes which is along the lines of this article would be to take

$$\Phi(\vec{x}) = M_1 \Phi_{\vec{v}_1}(\vec{x} - \vec{x}_1) + M_2 \Phi_{\vec{v}_2}(\vec{x} - \vec{x}_2),$$

where $\vec{v}_j$ are defined in a similar way as the $\vec{a}_j$ above. Whether or not this can easily be generalized to spinning black holes remains an open question.

For the case of two un-boosted Kerr black holes which have opposite angular momentum but which are equal in magnitude, we explicitly solved the constraint equations in the limit in which the black holes are close to each other. When solving the constraint equations, integration constants appear. These are associated with a deformation and a differential rotation of the apparent horizon. Although we have a geometrical picture for them, we do not know which values these constants will take in an astrophysical realistic collapse. It should be stressed that this is a generic problem of close limit calculations since realistic data can only be provided once the full 3D part of a black hole collision is solved. Fixing the integration constant to some specific value, we evolved the resulting distorted Schwarzschild black hole using the generalized Zerilli and RW equations in arbitrary coordinates and computed the radiated energy. Our result might change if the constants are chosen differently, but nevertheless, when compared to results with a different choice of initial slice, we found a qualitatively similar behavior of the radiated energy as a function of the angular momentum of the black holes. In particular, we confirmed that there is more energy radiated when the angular momentum of the black holes are parallel to the approaching axis.

A similar analysis to the one presented here, but for the far limit case, is already underway and will be helpful in giving us a clearer physical understanding of the parameters appearing in our initial data, in particular in view of

post-Newtonian calculations. Also, the physical meaning of our initial data in the intermediate region remains to be understood.

Finally, we plan to repeat our results using a version of the Teukolsky equation in horizon penetrating coordinates [15],[16] in order to test the latter and in order to proceed with more confidence to the case where the final black hole is a rotating one.

VII. ACKNOWLEDGMENTS

APPENDIX A: HARMONIC DECOMPOSITION

When expanding real quantities defined on the two-sphere S^2, it is convenient to work with the real spherical harmonics. In terms of the standard harmonics $Y^{\ell m}$, these are defined by

$$
\begin{aligned}
R^{\ell m} &= \frac{1}{\sqrt{2}} \left(Y^{\ell m} + Y^{\ell - m} \right), \\
I^{\ell m} &= \frac{1}{\sqrt{2}i} \left(Y^{\ell m} - Y^{\ell - m} \right).
\end{aligned}
$$

As the standard harmonics, the real harmonics defined here provide an orthonormal basis of square integrable functions on S^2.

For $\ell = 1$, we have

$$
\begin{aligned}
Y^{10} &= \sqrt{\frac{3}{4\pi}} \, \cos\theta, \\
R^{11} &= \sqrt{\frac{3}{4\pi}} \, \sin\theta \cos\phi, \\
I^{11} &= \sqrt{\frac{3}{4\pi}} \, \sin\theta \sin\phi.
\end{aligned}
$$

Note that with respect to this, the radial unit vector $\hat{x}$ can be written as $\hat{x} = \sqrt{4\pi/3}(R^{11}, I^{11}, Y^{10})$. For $\ell = 2$, the real harmonics are

$$
\begin{aligned}
Y^{20} &= \sqrt{\frac{5}{4\pi}} \frac{1}{2} \left(3\cos^2\theta - 1 \right), \\
R^{21} &= \sqrt{\frac{15}{4\pi}} \, \sin\theta \cos\theta \cos\phi, \\
I^{21} &= \sqrt{\frac{15}{4\pi}} \, \sin\theta \cos\theta \sin\phi, \\
R^{22} &= \sqrt{\frac{15}{16\pi}} \, \sin^2\theta \cos(2\phi), \\
I^{22} &= \sqrt{\frac{15}{16\pi}} \, \sin^2\theta \sin(2\phi).
\end{aligned}
$$

Choosing $\hat{e} = (0, \sin\chi, \cos\chi)$, and expanding the expressions for Φ and $\vec{b}$ given in (13,14) in terms of the harmonics

above, we obtain

$$\Phi = \frac{M}{r} + \frac{M\,M_1\,M_2}{r^3}\,\sqrt{4\pi}\left\{\frac{q^2}{3}Y^{00} + \frac{1}{\sqrt{5}}\left[1 + \frac{q^2}{6}(1 - 3\cos^2\chi)\right]Y^{20}\right.$$

$$\left. - \frac{1}{\sqrt{15}}\frac{q^2}{2}\left[2\sin\chi\cos\chi I^{21} - \sin^2\chi R^{22}\right]\right\}\epsilon^2 + \mathcal{O}(\epsilon^3),$$

$$\vec{b}\cdot d\vec{x} = -\frac{M\,M_1\,M_2}{r^3}\,q\,\sqrt{\frac{4\pi}{3}}\left\{\left[\frac{\cos\chi}{\sqrt{3}}Y^{00} + \sqrt{\frac{4}{15}}\cos\chi Y^{20} + \frac{\sin\chi}{\sqrt{5}}I^{21}\right]dr\right.$$

$$\left. + \frac{r}{2}\,\sin\chi\left[\frac{1}{\sqrt{5}}\,dI^{21} + \hat{*}dR^{11}\right] + \frac{r}{\sqrt{15}}\,\cos\chi\,dY^{20}\right\}\epsilon^2 + \mathcal{O}(\epsilon^3).$$

where $\hat{*}$ denotes the Hodge dual on S^2. Using the above expressions and rewriting Eq. (7) as

$$\vec{l}\cdot d\vec{x} = N\left(d\Phi + *d(\vec{b}\cdot d\vec{x})\right),$$

where $*$ denotes the Hodge dual on the three dimensional Euclidean space and N is chosen such that $\vec{l}$ is normalized, it is not difficult to find the expressions given in (15).

APPENDIX B: NUMERICAL EVOLUTION

Let us consider the following general one dimensional second order differential equation:

$$\partial_t^2 u + 2f_1\,\partial_t\partial_x u + f_2\,\partial_x^2 u + f_3\,\partial_t u + f_4\,\partial_x u + f_5\,u + f_6 = 0, \tag{B1}$$

with u and f_i functions of (t, x). We want to reformulate this equation as a system which is first order in time and space. To this purpose, we introduce the following new variable:

$$\pi = (\partial_t + g_+\,\partial_x)\,u,$$

with $g_\pm$ to be determined below. We have

$$(\partial_t + g_-\,\partial_x)\,\pi = \left\{\partial_t^2 + (g_+ + g_-)\,\partial_t\partial_x + g_+\,g_-\,\partial_x^2 + [(g_+)_{,t} + g_-\,(g_+)_{,x}]\,\partial_x\right\}u.$$

Comparing this last expression with Eq. (B1), we see that if

$$g_\pm = f_1 \pm \sqrt{f_1^2 - f_2}\,,$$

the original system (B1) assumes the form

$$\partial_{\mathbf{t}}\mathbf{v} = \mathbf{A}\partial_{\mathbf{x}}\mathbf{v} + \mathbf{B}\,\mathbf{v} + \mathbf{S}, \tag{B2}$$

with

$$\mathbf{v} = \begin{pmatrix} u \\ \pi \end{pmatrix}, \qquad \mathbf{A} = \begin{pmatrix} -g_+ & 0 \\ A_0 & -g_- \end{pmatrix}, \qquad \mathbf{B} = \begin{pmatrix} 0 & 1 \\ -f_5 & -f_3 \end{pmatrix}, \qquad \mathbf{S} = \begin{pmatrix} 0 \\ -f_6 \end{pmatrix},$$

where

$$A_0 = (g_+)_{,t} + g_-\,(g_+)_{,x} + f_3\,g_+ - f_4\,.$$

Applying the above to the equations (21,22), we find, in both cases,

$$g_+ = \frac{x-2}{x+2}\,, \qquad g_- = -1, \qquad A_0 = 0.$$

Since $\mathbf{A}$ is diagonal with real eigenvalues, the evolution system (B2) is strongly hyperbolic. One of the advantages of having a strongly hyperbolic system is that there is a well-defined way how to give boundary conditions (see, for example, [17]): u and π are characteristic modes with characteristic speeds $-g_+$ and $-g_-$, respectively. Inside the

horizon ($x < 2$), both speeds are positive which means that all modes leave the domain if we put the inner boundary inside the horizon. Thus, we can excise the singularity and extrapolate u and π at the inner boundary, which we put at $x < 2$. As long as $x > 2$, u is a mode with positive speed and π a mode with negative speed. At the outer boundary, we impose the outgoing wave condition $\pi = 0$.

We have written a code that numerically evolves (B2). This code is a second order accurate finite differencing one. Spatial derivatives are discretized using centered differencing and the time update is performed with an iterated Crank-Nicholson algorithm using two iterations. We have tested our code by comparing the resulting waveforms with the ones produced by the code used in Ref. [9]. We have calculated the quantities E_{even} and E_{odd} defined in Sec. V by integrating the Zerilli and Regge-Wheeler function, respectively, over time at a fixed location r_{obs} far away from the event horizon of the Schwarzschild background black hole. We have checked that the numerical results for E_{even} and E_{odd} at fixed r_{obs} converge as numerical resolution is increased and that these results do not change by more than 1.5% when r_{obs} is increased (with typical values of r_{obs} lying in the range $101M \leq r_{obs} \leq 151M$.)

[1] See the site http://ligo.caltech.edu, for the most recent advances on the LIGO.
[2] R. Price and J. Pullin, Phys. Rev. Lett. **72**, 3297 (1994); P. Anninos, R. Price, J. Pullin, E. Seidel, and W.-M. Suen, Phys. Rev. D **52**, 4462 (1995).
[3] G. Cook, Living Rev. Rel. **3**, 5 (2000).
[4] J.W. York Jr., J. Math. Phys., **14**, 456 (1973).
[5] A. Garat and R. H. Price, Phys. Rev. D **61**, 124011 (2000).
[6] N. T. Bishop, R. Isaacson, M. Maharaj, and J. Winicour, Phys. Rev. D **57**, 6113 (1998).
[7] R. A. Matzner, M. F. Huq and D. Shoemaker, Phys. Rev. D **59**, 024015 (1999).
[8] S. Dain, Phys. Rev. Lett. **87**, 121102 (2001).
[9] O. Sarbach, M. Tiglio, and J. Pullin, Phys. Rev. D **65**, 064026 (2002).
[10] G. Khanna, Phys.Rev. D **65**, 124018 (2002).
[11] O. Sarbach and M. Tiglio, Phys. Rev. D **64**, 084016 (2001).
[12] G. Khanna, Phys. Rev. D **63**, 124007 (2001).
[13] A. Ashtekar, C. Beetle, O. Dreyer, S. Fairhurst, B. Krishnan, J. Lewandowski, and J. Wisniewski, Phys. Rev. Lett. **85**, 3564 (2000); A. Ashtekar, C. Beetle, and J. Lewandowski, Class. Quantum Grav. **19**, 1195 (2002); Phys. Rev. D **64**, 044016 (2001).
[14] A. Ashtekar and B. Krishnana, *Dynamical horizons: energy, angular momentum, fluxes and balance laws*, gr-qc/0207080.
[15] C. Moreno and D. Núñez, Int. J. of Mod. Phys. D **11**, 1331 (2002).
[16] C. Moreno, D. Núñez, and O. Sarbach, in preparation.
[17] H. Kreiss and J. Lorentz, *Initial boundary value problems and the Navier Stokes equation*, Academic Press, San Diego, (1983).
[18] Here, we assume that the final black hole is a Kerr black hole.
[19] The radiated energy, being a coordinate invariant quantity, does not depend on this coordinate choice.
[20] A more precise way to calculate the angular momentum of the AH would be to use the corresponding formulas for an isolated horizon [13] or the newly introduced notion of dynamical horizon [14]. After linearizing the expressions in [13], we have obtain the same result as in Eq. (20).